Oxidation state of Ce in $Pb_2Sr_2Ce_{1-x}Ca_xCu_3O_8$

S. Skanthakumar and L. Soderholm
Chemistry Division and Intense Pulsed Neutron Source, Argonne National Laboratory, Argonne, Illinois 60439-4814
(Received 14 August 1995)

The structural and electronic properties of $Pb_2Sr_2Ce_{1-x}Ca_xCu_3O_8$ have been studied using neutron and x-ray diffraction, magnetization, and x-ray absorption near edge structure (XANES) experimental techniques. Our experiments show that although $Pb_2Sr_2Ce_{1-x}Ca_xCu_3O_8$ has the same crystal structure as any of the other $Pb_2Sr_2R_{1-x}Ca_xCu_3O_8$ (R=Y,Pr-Lu) compounds, superconductivity is not observed in the cerium-based materials. Neutron diffraction data also reveal an orthorhombic to monoclinic structural transition in $Pb_2Sr_2YCu_3O_8$ above room temperature, and this transition is expected to occur in other rare-earth $Pb_2Sr_2R_{1-x}Ca_xCu_3O_8$ materials also. Pr L_3-edge XANES measurements show that Pr is trivalent in $Pb_2Sr_2Pr_{1-x}Ca_xCu_3O_8$. In contrast, XANES measured on both the Ce L_3 and Ce K edges indicate that cerium is tetravalent in $Pb_2Sr_2R_{1-x}Ca_xCu_3O_8$. The valence of R is not affected by the Ca doping either for cerium or for any of the other rare-earth ions studied. Pb L_3 and Cu K edge XANES indicate that some of the extra charge introduced by cerium is transferred to the Cu-O layers responsible for the superconductivity changing Cu^{2+} to Cu^{1+}. This charge transfer may explain the absence of superconductivity in $Pb_2Sr_2Ce_{1-x}Ca_xCu_3O_8$.

I. INTRODUCTION

The effects on the physical properties of rare-earth (R) substitution for yttrium in $YBa_2Cu_3O_7$ have been studied using various experimental techniques. The superconducting properties of these materials are not affected by the rare-earth substitution[1] except for R=Ce, Pr, and Tb. Interestingly these are the only three f ions that have stable 4+ states. In the case of Tb or Ce, the $TbBa_2Cu_3O_7$ or $CeBa_2Cu_3O_7$ phases do not form. In contrast, $PrBa_2Cu_3O_7$ forms with the same crystal structure as $YBa_2Cu_3O_7$, but superconductivity is not observed in this material.[2,3] It has been suggested that the relative stability of tetravalent or intermediate-valent states of Ce, Pr, and Tb may be responsible for this exceptional behavior. However, recent experiments[4] on $Tb_{0.1}Y_{0.9}Ba_2Cu_3O_7$ confirm that the Tb ions are in the trivalent state. It has also been reported that the relative stability of $TbBaO_3$ inhibits the formation of $TbBa_2Cu_3O_7$ during the sample preparation process. Recent studies[3] on $PrBa_2Cu_3O_7$ indicate that Pr ions are also in the trivalent state. Hence this system does not give conclusive information about the rare-earth valence effects on the superconductivity.

An ideal system to study rare-earth valence effects on superconductivity is one in which all rare-earth ions from an isostructural series. Such a system is $Pb_2Sr_2RCu_3O_8$, in which all rare-earth ions, including Ce, Pr, and Tb, crystallize with similar fundamental structures.[5–12] In addition to superconductivity, this series shows a variety of very interesting rare-earth magnetic properties.[13–20] Superconductivity in these materials can be induced either by creating a sample with about 85% occupancy at the rare-earth site or by replacing 20–80 % of the trivalent rare-earth ion with divalent Ca. Once again, the exception is the R=Ce analog, which gives no indication of superconductivity at any Ca doping level.[5] In order to understand the influence of Ce on this system, we have performed neutron and x-ray diffraction, magnetization, and x-ray absorption near edge structure (XANES) experiments on $Pb_2Sr_2Ce_{1-x}Ca_xCu_3O_8$ and compared these results to those from similar experiments on $Pb_2Sr_2R_{1-x}Ca_xCu_3O_8$ (R=Y, Pr, and Tb). In this paper, we report the results of these experiments, which clearly demonstrate that Ce is tetravalent, in contrast to Tb and Pr, which are trivalent. The valences of the rare-earth ions or the Pb ion, which is 2+, are not affected by the Ca doping in this system. The Cu K-edge XANES data indicate that the extra charge introduced by Ce at least partially reduces the Cu, thereby affecting superconductivity.

II. EXPERIMENTAL DETAILS

Powder samples of $Pb_2Sr_2R_{1-x}Ca_xCu_3O_3$ (R=Y, Ce, Pr, and Tb) were prepared by solid-state reaction techniques. Initially, stoichiometric ratios of PbO, CuO, $CaCO_3$, $SrCO_3$, and Y_2O_3, $Ce_2(C_2O_4)_3\cdot 9(H_2O)$ (cerium oxalate), Tb_4O_7, or Pr_6O_{11} were mixed, pelletized, and prefired at 750 °C for 2 days. The samples were reground, pelletized again, and then sintered at 750 °C under a N_2 atmosphere for 2 days. This procedure was repeated until the x-ray diffraction data, which were taken on a Scintag θ-θ diffractometer (Cu $K\alpha$ radiation), showed the sample to be single phase.

Neutron diffraction measurements were performed on about 20 g samples at room temperature using the General-Purpose Powder Diffractometer (GPPD) at the Intense Pulsed Neutron Source (IPNS) at Argonne National Laboratory. The data were collected at three different mean detector angles of 148°, 90°, and 60°, which correspond to an instrumental resolution $\Delta d/d$ of about 0.0025, 0.005, and 0.01, respectively. Data in the d ranges of 0.5–2.9, 0.5–3.9, and 0.8–5.4 for 148°, 90°, and 60° detector banks, respectively, were analyzed simultaneously using the general structure analysis system (GSAS) program.[21]

The magnetization experiments were performed using a

TABLE I. Contributions to the XANES experimental resolutions that arise from instrument broadening and natural linewidths for the various edges studied. The percent change in calculated linewidths resulting from the convolution of the instrument broadening with the natural linewidth is also reported. All numbers reported are in units of eV.

Edge	Energy	Beam line	Natural width	Instrumental resolution width	Effective energy resolution	Percent (%) change
Pb L_3	13055	4-2	5.81	1.81	6.09	5
Ce K	40443	4-2	15.1	17.80	23.4	55
Ce L_3	5723	4-1	3.48	0.81	3.75	8
Pr L_3	5964	4-1	3.60	0.88	3.89	8
Cu K	8979	4-2	1.55	0.83	1.76	13

superconducting quantum interference device (SQUID) magnetometer over the temperature range of 10–320 K. Small pellets (100–300 mg) of powder samples were used for these experiments. In order check for superconductivity, small magnetic fields ($\leqslant$10 G) were employed, whereas magnetic susceptibilities were measured using an applied field of 500 G.

XANES experiments were conducted on powder samples at ambient temperature on the wiggler beam lines 4-1 and 4-2 at the Stanford Synchrotron Radiation Laboratory of Stanford University. Ce K-, Cu K-, and Pb L_3-edge data were collected on beam line 4-2, which was equipped with a Si(400) double-crystal monochromator that provides an energy resolution of $\delta E/E = 2.53\times10^{-5}$. Ce L_3- and Pr L_3-edge data were collected on 4-1, which is equipped with a Si(111) double-crystal monochromator that gives an energy resolution of $\delta E/E = 14.1\times10^{-5}$. 1 mm premonochromator vertical slits were used on both beam lines, and the monochromators were detuned by 50% to remove the higher-order harmonics. Under this configuration, the calculated instrumental energy bandwidth and its effect of the broadening on the natural width of XANES are given in Table I.[22,23] The method of data analysis is described elsewhere.[24]

III. RESULTS AND DISCUSSION

A. Neutron diffraction measurements

Neutron diffraction data were collected on several $Pb_2Sr_2R_{1-x}Ca_xCu_3O_8$ (R=Y, Ce, Pr, and Tb, x=0.0,0.5) samples at room temperature. We were able to prepare single-phase samples of $Pb_2Sr_2R_{1-x}Ca_xCu_3O_8$ only in the region of x=0.2–0.7. A few small additional peaks in the x=0.0 and 0.8 samples were attributable to other phases. A typical data set, on $Pb_2Sr_2Ce_{0.5}Ca_{0.5}Cu_3O_8$, is shown in Fig. 1. Several space groups, including tetragonal ($P4/mmm$),[6] orthorhombic ($Cmmm, Pman, Pmmm$),[7–10] and monoclinic ($C2/m, P2_1/m, P2_1$),[11,12] have been reported for this system. The observed reflections from our samples preclude a tetragonal unit cell, indicating instead that the crystal symmetry is orthorhombic or lower.

Our most reliable fit to the observed data was done in the orthorhombic space group $Cmmm$. Even though this symmetry gives a reasonably good fit overall, there are few notable discrepancies. First, we have observed several additional very weak reflections in all samples studied which can be indexed with the same orthorhombic cell. These additional reflections (h,k,l) satisfy the condition $h+k=2n+1$ and therefore are symmetry forbidden by the C-centering operation. Our temperature-dependent neutron diffraction experiments on $Pb_2Sr_2YCu_3O_8$ show that these peaks exist at all explored temperatures from 15 to 873 K. These weak peaks are not observable in x-ray diffraction experiments, suggesting that an additional component of oxygen ordering might be responsible for this C-centered violation. These extra very weak peaks can be indexed using the $Pman$ (Ref. 9)

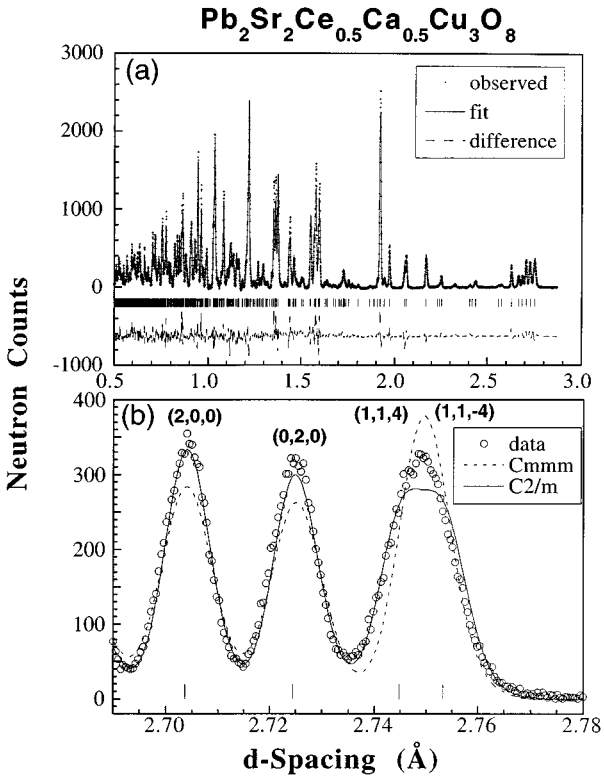

FIG. 1. Neutron diffraction data from $Pb_2Sr_2Ce_{1-x}Ca_xCu_3O$ at room temperature, obtained using 148° detector banks. The fit of the data to the $Cmmm$ orthorhombic space group is shown in (a). The true crystal symmetry of this compound is lower than $Cmmm$ (see text). The monoclinic $C2/m$ space group accounts for the broadening of selected peaks as shown in (b). The d spacings of the expected Bragg peaks are marked in (a) for the $Cmmm$ and in (b) for the $C2/m$ space group.

TABLE II. Lattice parameters and selected interatomic distances of $Pb_2Sr_2RCu_3O_8$. These data were obtained from refinements based on the space group *Cmmm*. The orthorhombic lattice constants (*a*, *b*, and *c*), cell volumes, and *R*-O distances are listed for various rare-earth samples. Numbers in parentheses represent errors in the last digit.

R	*a* (Å)	*b* (Å)	*c* (Å)	Volume (Å^3)	*R*-O (Å)
Y	5.3943(1)	5.4337(1)	15.7251(2)	460.93(1)	2.3989(1)
$Y_{0.5}Ca_{0.5}$	5.3789(2)	5.4184(2)	15.7454(5)	458.90(2)	2.4370(2)
Ce	5.4312(1)	5.4741(2)	15.8238(4)	470.45(2)	2.4857(2)
$Ce_{0.5}Ca_{0.5}$	5.4069(1)	5.4492(1)	15.7586(2)	464.30(1)	2.4413(1)
Pr	5.4449(1)	5.4836(1)	15.7982(3)	471.70(1)	2.4909(1)
$Pr_{0.5}Ca_{0.5}$	5.4016(2)	5.4457(2)	15.8002(6)	464.72(2)	2.5435(1)
Tb	5.4033(1)	5.4433(1)	15.7325(3)	462.72(1)	2.4213(1)
$Tb_{0.5}Ca_{0.5}$	5.3895(2)	5.4297(2)	15.7646(5)	461.33(2)	2.4438(2)

space group. Second, in addition to the extra weak reflections, some of the peaks such as the (1,1,4) are considerably broader than (2,0,0) or (0,2,0) peaks as demonstrated in Fig. 1(b). More generally for both the x-ray and neutron data, the (h,k,l) peaks with both h and $l \neq 0$ are broader than either the h or $l=0$ peaks. This systematic difference is consistent with a small monoclinic distortion (angle $\beta \neq 90°$) as reported earlier by several other groups.[11,12] Under this monoclinic distortion, the (h,k,l) peaks with both h and $l \neq 0$ are split into two peaks (h,k,l) and $(h,k,-l)$.

A refinement of our data using the monoclinic space group $C2/m$ (Ref. 11) is also shown in Fig. 1(b), and the refined angle β from this fit is 90.247(1)°. Even though our data are good enough to resolve peaks attributable to the monoclinic distortion, the data show significant peak broadening, but no splitting. This type of broadening has been previously observed in layered oxide systems, where it has been attributed to defects arising from stacking faults.[21,25] The poor statistics on the very weak reflections, together with the broadened line shapes for selected peaks, provided insufficient unique data to justify the added parameters required to obtain a good fit using a symmetry lower than *Cmmm*.

The above two deviations from *Cmmm* symmetry have been observed in all $Pb_2Sr_2R_{1-x}Ca_xCu_3O_8$ (R=Y, Ce, Pr, Nd, Tb, and Ho) compounds at room temperature with the β angle varying from 90.2° to 90.3°. Limited x-ray diffraction data in R=La, Sm, Eu, Dy, and Lu also gave indications for a monoclinic distortion.

Despite these difficulties, our refinements using the *Cmmm* space group are reliable enough to report *R*-O distances. In Fig. 1, we also include our fit using space group *Cmmm* (No. 65) (Ref. 7) and the difference between the fit and observed data. The lattice parameters and rare-earth–oxygen interatomic distances (*R*-O) obtained from this fit are given in Table II. Whereas we could discern no significant change in the oxygen content between Ce and other rare-earth compounds, problems with the details of our refinement preclude a quantitative conclusion. However, a clear understanding of the crystal structure is necessary in order to obtain accurate rare-earth and oxygen contents in our samples. Indeed, the observed line broadening may be an indication of defects or variations in oxygen content within one sample.

Our preliminary temperature-dependent neutron data on $Pb_2Sr_2YCu_3O_8$ provide some interesting information about the structure. The data at room temperature and 873 K are compared in Fig. 2. Like $Pb_2Sr_2Ce_{0.5}Ca_{0.5}Cu_3O_8$, this compound also may have a slight monoclinic distortion at room temperature [Fig. 2(a)]. However, when it was heated to high temperatures, the broad peaks narrowed, and the data were fit very well with the *Cmmm* space group as shown in Fig. 2(b). In contrast to the room-temperature data, the

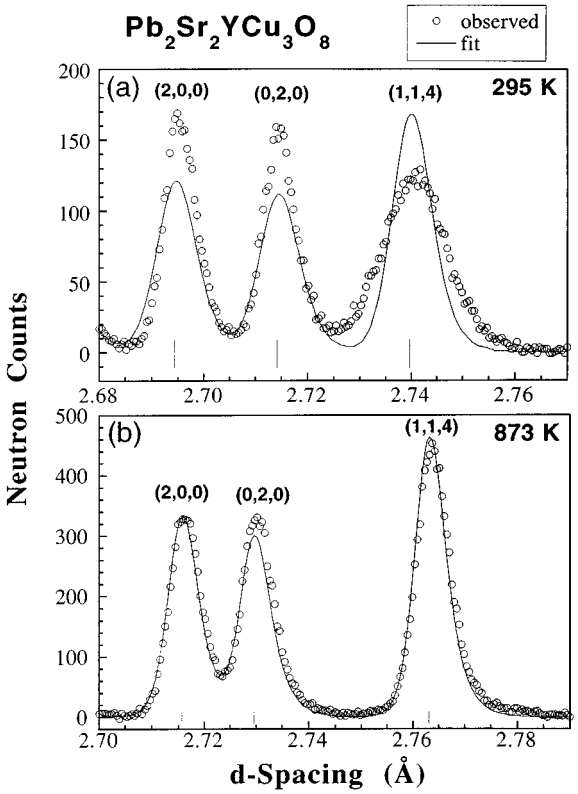

FIG. 2. Neutron diffraction data of $Pb_2Sr_2YCu_3O_8$ at (a) 295 K and (b) 873 K. The fit is to the *Cmmm* (orthorhombic) space group. The difference in intensities is mainly due to the different counting times. The width of (1,1,4) is larger than the (2,0,0) and (0,2,0) peaks at room temperature, whereas those widths are almost equal at 873 K. These observations are evidence for a monoclinic distortion that occurs when these compounds cooled to room temperature from high temperatures.

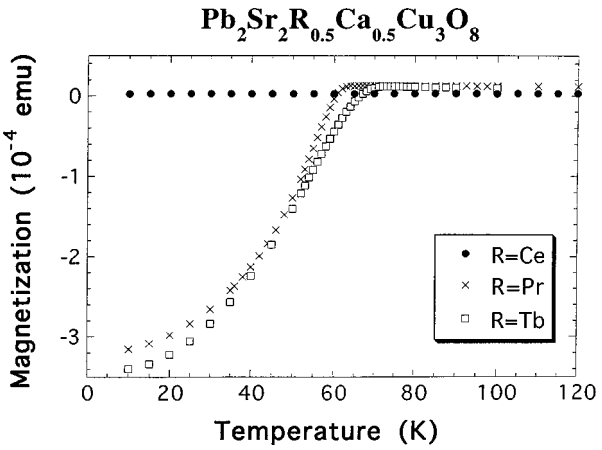

FIG. 3. Low-field ($\approx$10 G) magnetization vs temperature data obtained from polycrystalline compounds of $Pb_2Sr_2R_{0.5}Ca_{0.5}Cu_3O_8$ for R=Ce, Pr, and Tb. These data indicate superconductivity in R=Pr and Tb, whereas no evidence for superconductivity was found in Ce compounds down to 10 K.

(1,1,4) peak at 873 K has the same half width as the (2,0,0) and (0,2,0) reflections. The data at 473 and 673 K are similar to those obtained at 873 K, whereas the lower-temperature data are similar to those obtained at room temperature. Hence any orthorhombic-to-monoclinic structural distortion is expected to occur between 295 and 473 K. We suspect that a similar transition to an orthorhombic structure above room temperature occurs in all these compounds because all $Pb_2Sr_2R_{1-x}Ca_xCu_3O_8$ data showed selected peak broadening at room temperature.

B. Magnetization measurements

Magnetization data from $Pb_2Sr_2R_{0.5}Ca_{0.5}Cu_3O_8$ (R=Ce, Pr, and Tb), obtained as a function of temperature at low field, are shown in Fig. 3. These data clearly demonstrate superconductivity in the R=Pr and Tb compounds with transition temperatures above 60 K. Superconducting transition temperatures in this series are very sensitive to details of the sample preparations,[10] with T_c's as high as 84 K.[26] Our data on $Pb_2Sr_2Tb_{0.5}Ca_{0.5}Cu_3O_8$ are in contrast to a previous report,[27] in which superconductivity was not observed down to 15 K. In contrast to the Pr and Tb data, there is no evidence for superconductivity in $Pb_2Sr_2Ce_{0.5}Ca_{0.5}Cu_3O_8$ down to 10 K, although this compound was prepared in identical conditions to those for the Pr and Tb compounds. Our measurements on Ce samples with different Ce/Ca ratios, $0<x<0.8$, also showed no indication of bulk superconductivity. Our magnetic susceptibility data on $Pb_2Sr_2Ce_{1-x}Ca_xCu_3O_8$ were found to be similar to those of nonsuperconducting $Pb_2Sr_2YCu_3O_8$; that is, Ce in these compounds behaves like a nonmagnetic ion. This observation is taken as evidence that Ce is tetravalent, because the trivalent Ce (f^1) ion is magnetic ($\mu_{\text{eff}}=2.54\mu_B$), whereas tetravalent Ce (f^0) is diamagnetic, regardless of the crystal-field potential.

C. X-ray absorption near edge structure measurements

XANES is a single-ion probe that has been shown to be a powerful tool for determining valence states in complex systems.[28] The Pr L_3-edge XANES results on $Pb_2Sr_2PrCu_3O_8$ and superconducting $Pb_2Sr_2Pr_{0.5}Ca_{0.5}Cu_3O_8$ are compared in Fig. 4 with standard Pr^{3+} and Pr^{4+} compounds.The fingerprint of a Pr^{3+} spectrum (PrF_3) is a single resonance or white line centered at 5968 eV, whereas a Pr^{4+} spectrum (PrO_2) has two lines centered to higher energies 5971 and 5980 eV. XANES data on $Pb_2Sr_2Pr_{1-x}Ca_xCu_3O_8$ (x=0.0 and 0.5), shown in Fig. 4, exhibit only a single peak at 5968 eV. This observation demonstrates that the Pr is trivalent in these materials, and that the Pr valence is not affected by the Ca doping. This result is similar to a previous report,[15] in which it was demonstrated that the Tb ion is trivalent in $Pb_2Sr_2TbCu_3O_8$.

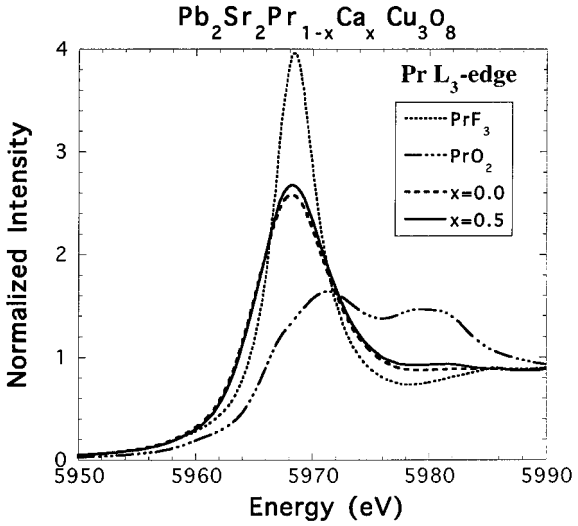

FIG. 4. Pr L_3-edge XANES data from PrF_3 (trivalent), PrO_2 (tetravalent), $Pb_2Sr_2PrCu_3O_8$, and superconducting $Pb_2Sr_2Pr_{0.5}Ca_{0.5}Cu_3O_8$ at room temperature. The fluorescence data are shown for $Pb_2Sr_2Pr_{1-x}Ca_xCu_3O_8$, while transmission data are shown for PrF_3 and PrO_2 as the thickness of the sample will strongly affect the fluorescence spectrum due to the high concentration of Pr. The similarity between the spectra obtained from $Pb_2Sr_2Pr_{1-x}Ca_xCu_3O_8$ and PrF_3 demonstrates that Pr in the Pb-based samples is trivalent.

XANES data on the Ce L_3 edges of $Pb_2Sr_2Ce_{1-x}Ca_xCu_3O_8$ (x=0.0 and 0.5) are compared with those of Ce^{3+} and Ce^{4+} standards as shown in Fig. 5. The fingerprint of a Ce^{3+} spectrum (CeF_3) is a single resonance or white line centered at 5728 eV, whereas a Ce^{4+} spectrum (CeO_2) has two lines centered to higher energies 5731 and 5738 eV. $Pb_2Sr_2Ce_{1-x}Ca_xCu_3O_8$ (x=0.0 and 0.5) XANES, shown in Fig. 5, have two peaks at 5731 and 5738, and are therefore similar to the data obtained from CeO_2. Hence, in contrast to other rare-earth ions, Ce is tetravalent in $Pb_2Sr_2Ce_{1-x}Ca_xCu_3O_8$. As seen from Fig. 5, the valence of Ce is not affected by Ca doping.

The observation of Ce^{4+} in $Pb_2Sr_2Ce_{1-x}Ca_xCu_3O_8$ is corroborated by Ce K-edge XANES data, which are shown together with those from Ce^{3+} and Ce^{4+} standards in Fig. 6. There is a shift in the absorption energies for trivalent (CeF_3) and tetravalent (CeO_2) Ce ions, as can be clearly observed from the first derivative of the intensities. The resonant energies for Ce^{3+} and Ce^{4+} are 40 466 and 40 473 eV, respectively. The Ce K-edge data on

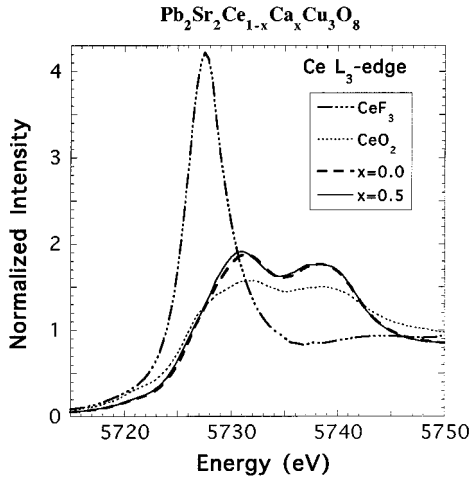

FIG. 5. Ce L_3-edge XANES spectra from CeF_3 (trivalent), CeO_2 (tetravalent), and $Pb_2Sr_2Ce_{1-x}Ca_xCu_3O_8$ ($x=0.0$ and 0.5). The fluorescence data are shown for $Pb_2Sr_2Ce_{1-x}Ca_xCu_3O_8$, whereas transmission data are shown for CeF_3 and CeO_2. The similarity between the spectra obtained from $Pb_2Sr_2Ce_{1-x}Ca_xCu_3O_8$ and CeO_2 demonstrates that Ce in the Pb-based samples is tetravalent.

$Pb_2Sr_2Ce_{0.5}Ca_{0.5}Cu_3O_8$ are also similar to those of CeO_2. Hence these experiments demonstrate that Ce is tetravalent in $Pb_2Sr_2Ce_{1-x}Ca_xCu_3O_8$.

Ce L_3- and K-edge XANES data show Ce to be tetravalent in this system, whereas XANES data on the other rare-earth ions, most notably Pr and Tb, indicate that they are trivalent. In trivalent rare-earth $Pb_2Sr_2RCu_3O_8$ compounds, the valences have been studied and are accepted as Pb^{2+}, Sr^{2+}, Cu^{+} (sandwiched by PbO), and Cu^{2+}-O (plane).[10] Holes, which are created by doping Ca^{2+} for R^{3+}, are thought to go into the CuO planes, convert the Cu^{2+} to Cu^{3+}, and thereby induce superconductivity.[10,29] The question then arises as to how the material compensates for the additional charge introduced when $R=$Ce. One possibility is

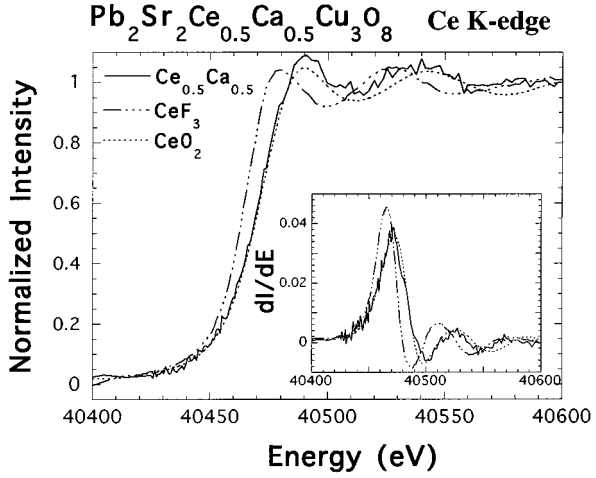

FIG. 6. Ce K-edge XANES results from CeF_3 (trivalent), CeO_2 (tetravalent), and $Pb_2Sr_2Ce_{0.5}Ca_{0.5}Cu_3O_8$ confirm the results from the Ce L_3-edge data. All these data were collected in transmission mode. The inset shows the first derivative of the intensities.

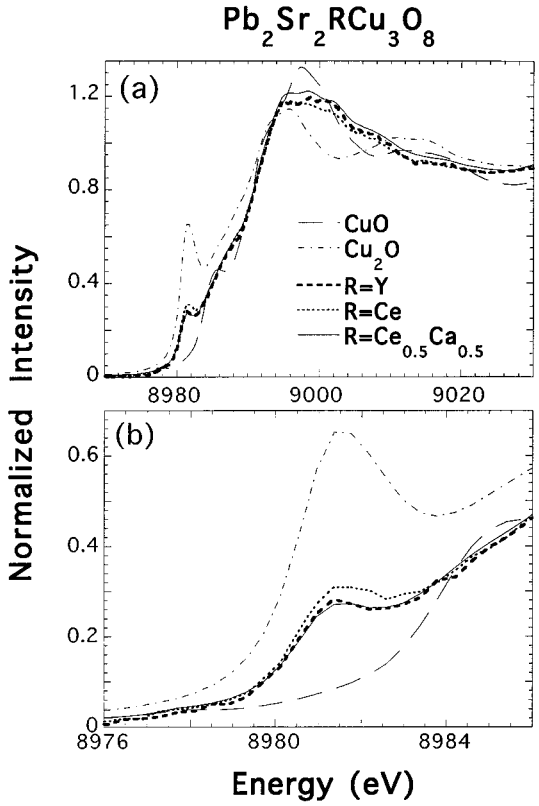

FIG. 7. Cu K-edge XANES results of Cu_2O (1+), CuO (2+), $Pb_2Sr_2Ce_{1-x}Ca_xCu_3O_8$ ($x=0.0$ and 0.5), and $Pb_2Sr_2YCu_3O_8$. All these data were collected using the electron-yield method of detection.

that the extra charge reduces another ion. In order to investigate this possibility, we have performed XANES experiments on Pb L_3 and Cu K edges of these materials.

Pb L_3-edge XANES experiments were conducted on $Pb_2Sr_2R_{1-x}Ca_xCu_3O_8$ ($R=$Y, Ce, and Pr), and the data were compared with those of Pb foil, divalent PbO, and tetravalent PbO_2. All spectra obtained from $Pb_2Sr_2R_{1-x}Ca_xCu_3O_8$, including the $R=$Ce compounds, were similar to those obtained from PbO. These results show that Pb in all these compounds is divalent and is affected neither by the presence of tetravalent Ce nor divalent Ca.

Representative Cu K-edge XANES results on $Pb_2Sr_2R_{1-x}Ca_xCu_3O_8$ ($R=$Y, Ce, Pr, and Tb) are shown in Fig. 7. Cu_2O (Cu^{+}) and CuO (Cu^{2+}) are used as standards. Cu^{+} has a pre-edge peak centered at about 8981 eV. This pre-edge peak is absent from higher valent Cu spectra, so that the relative magnitude of this pre-edge feature can be used as a quantitative estimate of the Cu^{+}/Cu^{2+} ratio present in a material. All measured $Pb_2Sr_2R_{1-x}Ca_xCu_3O_8$ spectra have a pre-edge peak at about 8981 eV, but it is weaker in intensity than in CuO. The presence of some Cu^{+} is consistent with both charge balance arguments and previous assertions that the Cu ions, sandwiched between PbO layers, are monovalent. The relative intensities of the Cu pre-edge feature for the Y- and Ce-based samples are shown in Fig. 7(b). An analysis of the data confirms that the peak from $Pb_2Sr_2CeCu_3O_8$ is slightly more intense than that obtained from $Pb_2Sr_2YCu_3O_8$, consistent with an in-

creased amount of Cu^+ in qualitatively $Pb_2Sr_2CeCu_3O_8$ over that in $Pb_2Sr_2YCu_3O_8$. This result demonstrates that at least some of the electrons introduced by Ce^{4+} are compensated by reducing some Cu^{2+} ions in the CuO planes to Cu^+. The Cu XANES data obtained from $Pb_2Sr_2Ce_{0.5}Ca_{0.5}Cu_3O_8$ are not significantly different from those of $Pb_2Sr_2YCu_3O_8$, and this can be observed in Fig. 7. These results indicate that if Ca^{2+} is doped for Ce^{4+} in this system, the extra charge will preferentially oxidize the planar Cu^+. Cu *K*-edge XANES in other trivalent $Pb_2Sr_2R_{1-x}Ca_xCu_3O_8$ (R=Y, Pr, and Tb, x=0.0 and 0.5) showed that Ca doping does not affect the Cu^+ concentration in the samples. It has been reported[10] that the extra holes created due to the Ca doping in the trivalent $Pb_2Sr_2R_{1-x}Ca_xCu_3O_8$ compound will go to the CuO planes and change Cu^{2+} to Cu^{3+}. This change will leave our pre-edge ratios unaffected.[30]

IV. DISCUSSION

All the powdered samples in the $Pb_2Sr_2R_{1-x}Ca_xCu_3O_8$ series (R=Y, Ce, Pr, and Tb) that were studied in this work are isostructural, as evidenced by x-ray and neutron diffraction. Whereas the true symmetry appears to be only pseudo orthorhombic, it was possible to get a consistent preliminary fit by assuming a higher, orthorhombic symmetry. From the chosen model, it is possible to discern the relative distances with enough reliability to establish trends as a function of R. These trends can be compared to the tabulated ionic radii of trivalent R,[31] which decrease monotonically with increasing Z, except for Y^{3+}, which is slightly smaller than Tb^{3+}. The ionic radius of Ce^{3+} is larger than that of the other trivalent rare earths studied, and hence the R-O distances and lattice constants are expected to be the largest for the Ce analog. In contrast to this expectation, the R-O distance, lattice parameter a,b, and the cell volume obtained from the pure Ce compound are smaller than those obtained from the corresponding Pr compound. However, assuming ratios of ionic radii, the Ce-O bond distances are not short enough to correspond to the presence of tetravalent Ce. The diffraction results indicate that the valence of Ce is higher than 3; however, it should be noted that the structures of these Pb-based materials are complicated and that the R-O distances are undoubtedly controlled by factors more complex than simply the size of R. Unfortunately, whereas the lattice constants and positional parameters obtained using orthorhombic symmetry are reliable, there are large uncertainties in the temperature factors and occupancies that preclude a meaningful comment on the oxygen content of the Ce analog relative to the other members of the series.

The question of the Ce valence is resolved by the L_3-edge XANES data, which clearly show that, in contrast to the other rare earths studied, Ce is tetravalent in $Pb_2Sr_2CeCu_3O_8$. There is no evidence for the presence of either trivalent or intermediate-valent Ce, either of which would be easily observable.[28] A comparison of the Cu XANES data taken from the R=Ce analog with those obtained from other trivalent R shows that there is a higher Cu^+ concentration in the Ce compounds. However, it is unclear, from either the Cu XANES or the neutron diffraction data, whether the excess charge introduced by the Ce^{4+} is compensated quantitatively by the reduction in Cu or whether there is some additional oxygen incorporated into the Ce compound. What is clear is that there is no appreciable change in the Pb-O sublattice and that all the Pb appears to remain divalent in the Ce analog. The incorporation of Ca into the samples, to form $Pb_2Sr_2Ce_{1-x}Ca_xCu_3O_8$, does not affect the Ce valence, but is seen to oxidize some of the Cu^+. From these data we conclude that the extra positive charge introduced into the Pb-Sr-Cu-based framework by Ce^{4+} is compensated by reducing some of the Cu^{2+} to Cu^+. The substitution of Ca^{2+} for Ce^{4+} serves to reoxidize some of the Cu^+ instead of oxidizing Cu^{2+} to produce the holes responsible for superconductivity.

The XANES results indicating the presence of Ce are further supported by the magnetic susceptibility data taken as a function of temperature. The data obtained from the Ce compound are very similar to those determined from the Y analog. Y is diamagnetic, as is Ce^{4+}, whereas Ce^{3+} (f^1 configuration) has an unpaired spin and a free-ion effective moment of $2.54\mu_B$. There is no evidence for the introduction of a local moment on Cu when R=Ce, consistent with the conclusion that the charge compensation produces Cu^+, which has no unpaired spins.

From the low-field magnetization data, it is determined that the Pr and Tb analogs of $Pb_2Sr_2R_{1-x}Ca_xCu_3O_8$ are superconducting, whereas the Ce analog, synthesized under similar conditions could not be made to superconduct. The absence of superconductivity in the Ce analog is attributed to the reduction of some planar Cu to Cu^+. The Ca doping merely reoxidizes some of the monovalent Cu to Cu^{2+} instead of creating some excess charge (Cu^{3+}) in the CuO planes. In principle, overdoping with Ca should produce the required carriers, but phase stability becomes a problem for Ca concentrations $x>0.7$. Attempts to induce superconductivity by making samples of $Pb_2Sr_2Ce_{1-\delta}\square_\delta Cu_3O_8$ ($\square$=vacancy) (Refs. 11, 32) also proved unsuccessful.

The absence of superconductivity in the $Pb_2Sr_2Ce_{1-x}Ca_xCu_3O_8$ phase is attributed to the disruption of the CuO planar electronic states that results directly from charge transfer induced by the incorporation of tetravalent Ce. Whether the effect of the charge transfer on superconductivity is augmented by subtle hybridization effects similar to those proposed for Pr in $PrBa_2Cu_3O_7$ (Ref. 33) remains unclear. The observation of superconductivity in the Pr analog of the $Pb_2Sr_2R_{1-x}Ca_xCu_3O_8$ series indicates that there may be subtle differences in hybridization effects in this series, as compared to the $RBa_2Cu_3O_7$ series, that are not currently understood.

ACKNOWLEDGMENTS

We thank Mark R. Antonio, J. W. Richardson, Jr., and U. Welp for their technical assistance. We also thank U. Staub for useful discussions. This research is supported by the Department of Energy, Basic Energy Sciences, Chemical Sciences and Materials Sciences, under Contract No. W-31-109-ENG-38. SSRL is operated by the Department of Energy, Office of BES.

[1] P. H. Hor, R. L. Meng, Y. Q. Wang, L. Gao, Z. J. Huang, J. Bechtold, K. Forster, and C. W. Chu, Phys. Rev. Lett. **58**, 1891 (1987).
[2] L. Soderholm, K. Zhang, D. G. Hinks, M. A. Beno, J. D. Jorgensen, C. U. Segre, and I. K. Schuller, Nature **328**, 604 (1987).
[3] H. B. Radousky, J. Mater. Res. **7** 1917 (1992).
[4] U. Staub, M. R. Antonio, L. Soderholm, M. Guillaume, W. Henggeler, and A. Furrer, Phys. Rev. B **50**, 7085 (1994).
[5] L. F. Schneemeyer, R. J. Cava, A. C. W. P. James, P. Marsh, T. Siegrist, J. V. Waszczak, J. J. Krajewski, W. P. Peck, Jr., R. L. Opila, S. H. Glarum, J. H. Marshall, R. Hull, and J. M. Bonar, Chem. Mater. **1**, 548 (1989).
[6] M. A. Subramanian, J. Gopalakrishnan, C. C. Torardi, P. L. Gai, E. D. Boyes, T. R. Askew, R. B. Flippen, W. E. Farneth, and A. W. Sleight, Physica C **157**, 124 (1989).
[7] R. J. Cava, M. Marezio, J. J. Krajewski, and W. F. Peck, Jr., Physica C **157**, 272 (1989).
[8] J.-E. Jørgensen and N. H. Andersen, Acta Chem. Scand. **45**, 19 (1991).
[9] C. Chaillout, O. Chmaissen, J. J. Capponi, T. Fournier, G. McIntyre, and M. Marezio, Physica C **175**, 293 (1991).
[10] M. Marezio, A. Santoro, J. J. Capponi, E. A. Hewat, R. J. Cava, and F. Beech, Physica C **169**, 401 (1990).
[11] J. S. Xue, J. E. Greedan, and M. Maric, J. Solid State Chem. **102**, 501 (1993).
[12] H. Fujishita, M. Sato, Y. Morii, and S. Funahashi, Physica C **210**, 529 (1993).
[13] L. Soderholm, C.-K. Loong, J. S. Xue, J. P. Hammonds, J. E. Greedan, and M. Maric, J. Appl. Phys. **73**, 6314 (1993).
[14] L. Soderholm, C.-K. Loong, U. Staub, S. Skanthakumar, J. S. Xue, J. P. Hammonds, J. E. Greedan, and M. Maric, Physica C **246**, 11 (1995).
[15] U. Staub, L. Soderholm, S. Skanthakumar, and M. R. Antonio, Phys. Rev. B **52**, 9736 (1995).
[16] S. Y. Wu, W. T. Hsieh, W.-H. Li, K. C. Lee, J. W. Lynn, and H. D. Yang, J. Appl. Phys. **75**, 6598 (1994).
[17] W. T. Hsieh, W-H. Li, K. C. Lee, J. W. Lynn, J. H. Shieh, and H. C. Ku, J. Appl. Phys. **76**, 7124 (1994).
[18] J. H. Shieh, H. C. Ku, and J. C. Ho, Phys. Rev. B **50**, 3288 (1994).
[19] C. R. Shih, T. H. Meen, Y. C. Chen, and H. D. Yang, Phys. Rev. B **50**, 9619 (1994).
[20] H. C. Ku, C. C. Lai, J. H. Shieh, J. W. Liou, C. Y. Wu, and J. C. Ho, Physica B **194**, 213 (1994).
[21] A. C. Larson and R. B. Von Dreele (unpublished).
[22] M. O. Krause and J. H. Oliver, J. Phys. Chem. Ref. Data **8**, 329 (1979).
[23] A. E. Sandström, in *Handbuch Der Physik*, edited by S. Flügge (Springer-Verlag, Berlin, 1957), Vol. 30, p. 78.
[24] F. W. Lytle, in *Applications of Synchrotron Radiation*, edited by H. Winick, D. Xian, M. H. Ye, and T. Huang (Gordon and Breach, New York, 1989), Vol. 4, p. 135.
[25] J. S. Xue, M. R. Antonio, and L. Soderholm, Chem. Mater. **7**, 333 (1995).
[26] J. S. Xue, M. Reedyk, Y. P. Lin, C. V. Stager, and J. E. Greedan, Physica C **166**, 29 (1990).
[27] J.-E. Jørgensen and N. H. Anderson, Physica C **235**, 877 (1994).
[28] J. Röhler, in *Handbook on the Physics and Chemistry of Rare Earths*, edited by K. A. Gschneidner, L. Eyring, and S. Hüfner (North-Holland, Amsterdam, 1987), Vol. 10, p. 453.
[29] L. F. Mattheiss and D. R. Hamann, Phys. Rev. B **39**, 4780 (1989).
[30] E. E. Alp, L. Soderholm, G. K. Shenoy, D. G. Hinks, B. W. Veal, and P. A. Montano, Physica B **150**, 74 (1988).
[31] R. D. Shannon, Acta Crystallogr. A **32**, 751 (1976).
[32] J. S. Xue, M. Reedyk, J. E. Greedan, and T. Timusk, J. Solid State Chem. **102**, 492 (1993).
[33] L. Soderholm, C.-K. Loong, G. L. Goodman, and B. D. Dabrowski, Phys. Rev. B **43**, 7923 (1991).